Retina

Evaluating Contrast Sensitivity in Early and Intermediate Age-Related Macular Degeneration With the Quick Contrast Sensitivity Function

Philipp Anders,[1–4] Ghislaine L. Traber,[1] Ursula Hall,[1] Simona A. Garobbio,[5] Eric J. Chan,[1] Chrysoula Gabrani,[1] Hanna Camenzind,[2] Maximilian Pfau,[1,2] Michael Herzog,[5] and Hendrik P. N. Scholl[1,2]

[1]Institute of Molecular and Clinical Ophthalmology Basel, Basel, Switzerland
[2]Department of Ophthalmology, University of Basel, Basel, Switzerland
[3]Ophthalmology Unit, Centro Hospitalar e Universitário de Coimbra (CHUC), Coimbra, Portugal
[4]AIBILI, Association for Innovation and Biomedical Research on Light and Image, Coimbra, Portugal
[5]Laboratory of Psychophyics, École polytechnique fédérale de Lausanne (EPFL), Lausanne, Switzerland

Correspondence: Hendrik P. N. Scholl, Institute of Molecular and Clinical Ophthalmology Basel, Mittlere Strasse 91, Basel 4031, Switzerland; hendrik.scholl@iob.ch.

Received: May 17, 2023
Accepted: October 15, 2023
Published: November 7, 2023

Citation: Anders P, Traber GL, Hall U, et al. Evaluating contrast sensitivity in early and intermediate age-related macular degeneration with the quick contrast sensitivity function. *Invest Ophthalmol Vis Sci*. 2023;64(14):7. https://doi.org/10.1167/iovs.64.14.7

Purpose. The purpose of this study was to describe, validate, and compare the contrast sensitivity functions (CSFs) acquired with the novel quick CSF (qCSF) method from patients with early and intermediate age-related macular degeneration (eAMD and iAMD) and healthy controls.

Methods. This is a cross-sectional analysis of contrast sensitivity (CS) and visual acuity (VA) baseline data from the prospective Multimodal Functional and Structural Visual System Characterization (MUMOVI) study. The qCSF testing was conducted with the manifold contrast vision meter (Adaptive Sensory Technology, San Diego, CA, USA). CS levels at spatial frequencies from 1 cycle per degree (CPD) to 18 CPD, the area underneath the logarithmic contrast sensitivity function (AULCSF), and contrast acuity (CA) were analyzed. The association of functional metrics with variables of interest was tested with linear models.

Results. Ninety-four study eyes from 94 study patients were included in the analysis (13 patients with eAMD, 33 patients with iAMD, and 48 healthy controls). Significant differences between the eAMD and the iAMD model estimates were only found for CS at 1 CPD (t value = −2.9, P value = 0.006) and CS at 1.5 CPD (−2.7, 0.01). A specific association between smoking years and CS at 1 CPD (P = 0.02) and CS at 1.5 CPD (P = 0.03) could be described in patients with AMD.

Conclusions. The qCSF testing allows the fast measurement of the whole CSF, enabling the integration into clinical routine. We showed that novel qCSF-derived metrics detect slight functional differences between AMD stages, which testing by Pelli-Robson charts or VA testing would miss. This study, therefore, yields novel qCSF-derived candidate metrics for therapeutic trials in AMD.

Keywords: age-related macular degeneration (AMD), quick contrast sensitivity function (qCSF), lower spatial frequencies, candidate functional markers

Age-related macular degeneration (AMD) predominantly disturbs the patients' central vision and therefore strongly disrupts their visual capacities. The worldwide prevalence of AMD is estimated to be at 300 million by 2040.[1] In the evaluation of therapeutic strategies for AMD, adequate end points are essential. In spite of the quantitative advantages of imaging-derived morphologic metrics,[2–4] regulatory agencies have emphasized the role of functional outcome measures, which determine the clinical relevance of treatment effects for the patients.[5] To this end, the metrics of best-corrected visual acuity (BCVA), low-luminance visual acuity (LLVA), and microperimetry (MP) have been studied extensively in the context of AMD.[6–13] BCVA and LLVA measure the spatial resolution of the visual system, that is, these tests ask for the smallest detail of high contrast, that can be detected. MP tests the retinal sensitivity for relatively small light stimuli across the macula. Of note, due to their design, the aforementioned tests omit an important component of visual performance: contrast sensitivity (CS). Briefly, the ability to see delicate objects does not guarantee the ability to see large or medium-sized objects of low contrast.[14] A metric that incorporates both visual acuity i.e. spatial resolution) and CS is the contrast sensitivity function (CSF).

To measure spatial resolution, the stimulus size is resolved along a sinusoidal grating pattern and quantified in cycles of grating pattern per degree of visual angle (cycles

Investigative Ophthalmology & Visual Science

per degree [CPD]), where one cycle consists of one light bar and one dark bar. Contrast is defined by the difference between the maximum luminance of the light bar and the minimum luminance of the dark bar as follows: $C = (L_{max} - L_{min})/L_{min}$. Consequently, the response of interest, which is inquired from the patient, is the contrast threshold at a certain spatial frequency, that is, the minimum amount of contrast, which is needed to detect the presence of a spatially patterned stimulus. Contrast thresholds are measured for gratings of various spatial frequencies. The reciprocal of contrast threshold is CS. The CS is plotted against spatial frequency (in CPD), which yields the CSF.[14] The relation of visual acuity to the CSF is the following: Visual acuity is equivalent to the point, where the CSF curve meets the x-axis at the highest resolvable spatial frequency, which is at the lowest CS, that is, at the highest contrast level. For example, a logMAR Early Treatment Diabetic Retinopathy Study (ETDRS) visual acuity of 0 corresponds to a spatial grating of 30 cycles per degree, which features a bar width of 1 minute of the arc. In conclusion, measuring the CSF as opposed to only measuring visual acuity, provides a wide range of additional information on visual performance. In the context of AMD, CS has been shown to correlate with morphologic metrics in neovascular AMD[15] and with advancing stages of dry AMD.[16]

Traditionally CS is measured manually with Pelli-Robson charts.[17] Another established method to measure CS is the presentation of Gabor patches on a computer screen.[18–20] Both approaches above, however, are usually only used to determine CS at selected spatial frequencies (between 3 CPD and 5 CPD), because 500 to 1000 trials of CS at different spatial frequencies would be needed in these methods for a full CSF, which could take up to 60 minutes for one patient.[21] A new approach, which delivers precise CSFs within less than 10 minutes is the computer-based quick CSF method (qCSF), which uses Bayesian inference to collect data points around predicted patient-specific CSFs.[22] After reviewing several parametric functions, the authors decided to characterize the CSF as truncated log-parabola by four parameters: peak gain, peak frequency, bandwidth, and truncation at the low frequency side. These four parameters are directly estimated using Bayesian adaptive inference.

In this cross-sectional analysis of baseline data from the longitudinal Multimodal Functional and Structural Visual System Characterization (MUMOVI) study, we examined CSFs acquired with the qCSF method on patients with early AMD (eAMD), intermediate AMD (iAMD) and healthy controls and compared the outputs of the different groups. Further, we analyzed the sensitivity of CS metrics, BCVA, and LLVA toward eAMD and iAMD. Of interest, in persons with eAMD and iAMD, smoking has been reported to be associated with the progression to advanced AMD.[23] To this end, we also studied the association of CS metrics, BCVA, and LLVA with smoking years, in order to see whether visual performance is influenced by smoking behavior in eAMD and iAMD. Finally, we evaluated the association of qCSF-derived metrics with contrast thresholds as determined by the presentation of Gabor patches.

Methods

Participants

This is a cross-sectional analysis of the prospective natural history cohort study termed MUMOVI, performed at a tertiary referral center (University Hospital Basel, PI: Prof. Dr. med. Hendrik P.N. Scholl), in cooperation with the École polytechnique fédérale de Lausanne (EPFL). The clinical protocol adhered to the Declaration of Helsinki and was approved by the institutional review board (Swiss Ethics No. 2021-00029). Written consent was provided by all participants prior to enrollment in the study.

Forty-nine participants with AMD and 50 healthy controls were recruited from general and retinal ophthalmologic clinics in the University Eye Hospital Basel between June 2021 and June 2022. The study featured a baseline visit and follow-up visits at months 12 and 24. Important inclusion criteria for the AMD group were (1) clinical diagnosis of AMD, (2) age $\geq$ 50 years, (3) media clarity, and (4) good pupillary dilatation. The AMD staging was conducted according to the Beckman classification[24] by two trained physicians (authors H.C. and P.A.): eAMD – medium drusen > 63 µm and $\leq$ 125 µm and no pigmentary abnormalities; iAMD – large drusen > 125 µm and/or any pigmentary abnormalities; advanced AMD – neovascular AMD and/or any geographic atrophy. The exclusion criteria comprised ocular disease, other than AMD, affecting visual function or ocular morphology. Healthy non-dominant control eyes apart from refractive error or prior cataract surgery were enrolled with participants aged $\geq$ 50 years. The inability to perform all ophthalmic and psychophysical examinations constituted an exclusion criterium for both study groups. At every visit, a slit lamp examination, a medical history assessment, and the Mechanism of Coordinated Access (MoCA) test,[25] were conducted. Further, the following ophthalmologic examinations were run at every visit: BCVA, LLVA, MP, qCSF, macula and retinal nerve fiber layer (RNFL) optical coherence tomography (OCT) Spectralis. Finally, a custom psychophysiological test battery on an LCD screen was presented at every visit, comprising the following elements: motion discrimination, Freiburg visual acuity test, orientation discrimination, visual search, and CS testing with Gabor patches. In the following, the tests with relevance to this publication will be described in detail.

Testing

Visual acuity was determined by using the ETDRS visual acuity charts at 4 meters, with the best refractive correction. The LLVA was measured by covering the best-corrected study eye with a 2.0-log unit neutral density filter and then repeating the visual acuity evaluation. The test chart luminance of 130 candela/m^2 was maintained throughout both visual acuity examinations.

CS testing with Gabor patches was conducted as part of a psychophysiological test battery with best refractive correction. The stimuli were presented on an LCD screen at 2 m in a room with standardized illumination. Participants were tested monocularly and gave their responses by pushing buttons on a hand-held wireless control. The participants needed to discern whether the Gabor patch was oriented clockwise or anticlockwise compared to vertical. The orientation was modified by 45 degrees. The Gabor patch had a spatial frequency of 3 CPD and a diameter of 3 arcdeg. The stimulus was presented for 200 ms. The mean luminance was 50%. An auditory feedback tone was provided after incorrect responses. An annulus at a luminance of 70% around the Gabor patch indicated when it was potentially presented. Test levels were chosen following the QUEST adaptive procedure working on a logarithmic

scale.[26] The outcome was the contrast level, for which 75% of correct responses were given. Contrast threshold (CT) and CS, the reciprocal, were reported as appropriate. A graphical illustration of the Gabor CS testing procedure has been published by Tibber et al.[19]

The qCSF testing was conducted in the same room at standardized illumination of approximately 7 lux with the manifold contrast vision meter (Adaptive Sensory Technology, San Diego, CA, USA) and with best refractive correction. The device presents triples of Sloan letters with > 300 possible contrast levels at spatial frequencies ranging from 1 CPD to 27 CPD on an LED monitor. The participants were asked to read the presented optotypes and their responses were registered (as correct, incorrect, or optotype not seen) on a tablet computer by a trained study nurse. The following metrics were exported from the qCSF platform: the contrast acuity (CA) in logCPD, the point in which the CSF curve meets the x-axis at the highest resolvable spatial frequency and at the lowest CS; the CS values at spatial frequencies 1 CPD, 1.5 CPD, 3 CPD, 6 CPD, 12 CPD, and 18 CPD, and the area underneath the logarithmic contrast sensitivity function (AULCSF) in logCS. A graphical illustration of the qCSF testing procedure has been published by Traber et al.[27]

Statistical Analysis

Microsoft Excel (Microsoft Corporation, Redmond, WA, USA), GraphPad Prism (GraphPad Software, San Diego, CA, USA) and the software environment R[28] with add-on packages lme4 and sjPlot were used for statistical analysis. Data were assessed for Gaussian normal distribution by the D'Agostino and Pearson test and parametric or nonparametric statistics were calculated as appropriate. ANOVA and multiple-comparison tests were used to compare the cohort characteristics. In this study, multiple multivariable linear regression models were built and used for analysis. In these models, the respective functional metrics (BCVA, LLVA, Gabor CS, CA, AULCSF, and CS thresholds) were consistently input as dependent variables and variables of interest (AMD stage by Beckman Classification,[24] lens status, and smoking years always in combination with age) were introduced as a fixed effect. In specifics, age was found to be significantly associated with all tested functional metrics in this dataset. Consequently, age was included in linear regression models in order to control for its effect on the dependent variables. In the case at hand, the effect of the continuous variable age on the dependent variables can be assumed to be reproducible in other cohorts. Therefore, age was introduced as a fixed effect.[29,30] A univariable linear model with CS at 1 CPD as the dependent variable and smoking years as a fixed effect was fitted to retrieve the respective regression line. Hypothesis tests were performed using a 5% (0.05) significance level. For normally distributed data, mean and standard deviation (SD) are presented and for not normally distributed data median and interquartile range (IQR) are presented.

Results

Cohort Characteristics

This baseline analysis of functional data from the MUMOVI study included 94 study patients with one study eye each. Of the total 99 study eyes enrolled in the MUMOVI study, 5 eyes were excluded from this analysis due to insufficient CS data quality or divergent AMD stage. In specifics, 48 control eyes, 13 eAMD eyes, and 33 iAMD eyes were analyzed (Table 1). There was a significant age difference between the control and eAMD groups ($P = 0.004$) and the control and iAMD groups ($P < 0.0001$), whereas the age between AMD groups showed no significant difference ($P = 0.6$). As all tested functional metrics were found to be significantly associated with age ($P < 0.001$), age was controlled for by including it as a fixed effect in subsequent regression analyses. The control group was female-dominated (62.5%) with a balanced right-to-left eye ratio. The AMD groups overall included an equal number of female and male eyes and a higher percentage of right eyes (63%). The study participants were White except for one participant in the iAMD group and there were more phakic eyes than pseudophakic eyes included in the control group (89.6%), eAMD group (92.3%), and iAMD (63.6%) group. However, univariate linear regression analysis revealed no significant association of lens status with any of the tested functional metrics.

Comparison of Functional Metrics Between Healthy Controls and AMD Subgroups

Multivariate linear regression analysis of functional metrics with the Beckman AMD classification (eAMD and iAMD)

Table 1. Demographic Data of the Study Population

Subject No.	Parameter	Control	eAMD	iAMD	AMD Combined
1	No. of patients and study eyes	48	13	33	46
2	Mean age (SD)	66 (8.5)	74 (6.0)	75 (7.2)	74 (6.8)
3	Sex				
	Female	30 (62.5%)	5 (38.5%)	18 (54.5%)	23 (50%)
	Male	18 (37.5%)	8 (61.5%)	15 (45.5%)	23 (50%)
4	Eye				
	Right	23 (47.1%)	10 (77.0%)	19 (57.6%)	29 (63%)
	Left	25 (52.1%)	3 (23.0%)	14 (42.4%)	17 (37%)
5	Race				
	White	48 (100%)	13 (100%)	32 (97.0%)	45 (97.8%)
	Other	0 (0%)	0 (0%)	1 (3.0%)	1 (2.2%)
6	Lens status				
	Phakic	43 (89.6%)	12 (92.3%)	21 (63.6%)	33 (71.7%)
	Pseudophakic	5 (10.4%)	1 (7.7%)	12 (36.4%)	13 (28.3%)
7	Median smoking years (IQR)	0 (0-17.5)	8 (0-21)	14 (0-26.5)	9.5 (0-22.8)

Table 2. Age-Controlled Comparison of Functional Metrics Between eAMD and iAMD Subgroups

Variable	eAMD Model Estimate [95% CI]	iAMD Model Estimate [95% CI]	*T* Value	*P* Value
BCVA (logMAR)	−0.39 [−0.72 to −0.07]	−0.37 [−0.76 to −0.02]	0.7	0.5
LLVA (logMAR)	−0.19 [−0.58 to −0.21]	−0.18 [−0.65 to −0.30]	0.3	0.8
CS Gabor 3 cpd (logCS)	2.62 [1.33–3.91]	2.43 [0.87–3.99]	−1.4	0.2
Metrics deduced from qCSF method				
CA (logCPD)	1.76 [1.33–2.20]	1.71 [1.20–2.24]	−1.1	0.3
AULCSF (logCS•logCPD)	2.15 [1.35–2.94]	2.05 [1.09–3.0]	−1.3	0.2
CS at specific spatial frequencies				
1 cpd (logCS)	1.91 [1.46–2.36]	1.78 [1.24–2.32]	−2.9	**0.006**
1.5 cpd (logCS)	2.11 [1.65–2.58]	1.99 [1.44–2.55]	−2.7	**0.01**
3 cpd (logCS)	2.32 [1.66–2.98]	2.22 [1.43–3.01]	−1.5	0.1
6 cpd (logCS)	2.10 [1.18–3.01]	2.01 [0.91–3.10]	−1.0	0.3
12 cpd (logCS)	1.61 [0.56–2.66]	1.53 [0.27–2.78]	−0.8	0.4
18 cpd (logCS)	0.90 [0.12–1.67]	0.85 [−0.08 to −1.78]	−0.6	0.5

and age as fixed effects only showed significant differences between the eAMD and the iAMD model estimates for CS at 1 CPD (t value = −2.9, P value = 0.006) and CS at 1.5 CPD (−2.7, 0.01; Table 2). Other qCSF-derived metrics, Gabor CS, and visual acuity metrics did not show a significant difference between eAMD and iAMD. Comparing the control and eAMD model estimates no tested metric exhibited significant differences (Supplementary Table S1). All qCSF-derived metrics and the Gabor CS showed significant differences between the control and iAMD model estimates, whereas the BCVA and LLVA model estimates were not significantly different (Supplementary Table S2). Over all tested groups, CA was significantly associated with BCVA and LLVA (P < 0.001). For reference the results from non-age-controlled models are included in the supplementary materials (Tables S4–S6).

Contrast Sensitivity Functions in eAMD, iAMD, and Controls

The median CSF (Fig. 1) for iAMD showed lower contrast sensitivities than the eAMD and the control group at lower spatial frequencies (1 CPD and 1.5 CPD) with a limited overlap of the IQRs. At these lower spatial frequencies, the eAMD median CSF was similar to the control CSF with overlying IQRs. Starting from 3 CPD, the IQRs of the AMD groups predominantly overlap, and at 6 CPD the eAMD CSF was closest to the iAMD CSF. At 6 CPD and 12 CPD the eAMD median CSF showed the greatest negative deviation from the control group.

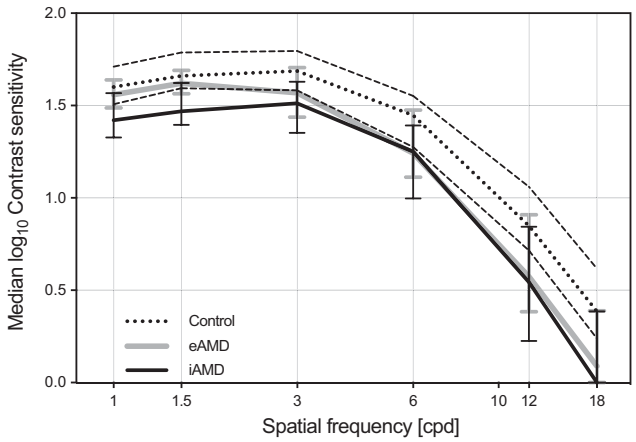

Figure 1. Median contrast sensitivity functions. IQRs are plotted as whiskers for eAMD and iAMD and as dashed lines for control. Spatial frequency is plotted on a log10 scale.

Association of qCSF Metrics With Contrast Thresholds Measured With Gabor Patches

Multivariate linear regression analysis provided significant associations (P < 0.001) of all measured qCSF metrics with CTs assessed by Gabor patches. In addition, LLVA (P < 0.001) and BCVA (P = 0.02) were significantly associated with Gabor CTs. Best model fitting as evaluated by coefficients of determination was achieved in the model including CS at 3 CPD as the dependent variable (R^2/adjusted R^2: 0.689/0.682). The CS at 1 CPD yielded the lowest coefficients of determination among the qCSF-derived metrics (0.296/0.279). Models with LLVA (0.342/0.326) and BCVA (0.208/0.189) as the dependent variables also showed lower coefficients of determination. See Supplementary Table S3 for a full list of model intercept, slope, R^2, and adjusted R^2.

Association of Contrast Sensitivity With Smoking

Multivariate linear regression analysis with smoking years as a fixed effect did not show a significant correlation with any CS metric in the control group. However, in patients with AMD (eAMD and iAMD groups combined; see Table 3, Fig. 2) there was a significant association for CS at 1 CPD (P = 0.02) and CS at 1.5 CPD (P = 0.03) with smoking years. In contrast, other qCSF-derived metrics like AULCSF (P = 0.6) or VA metrics like BCVA (P = 0.7) did not show a significant correlation with smoking years.

Discussion

This cross-sectional analysis of MUMOVI baseline data explored the evaluation of CS in eAMD, iAMD, and healthy controls with the qCSF method.[22] The study showed no significant differences for all tested functional metrics (visual acuity and CS) between the control and eAMD groups. Comparing the control and iAMD groups all CS metrics, but no visual acuity metric, showed a significant difference

Table 3. Association of Visual Function Metrics With Smoking Years in Patients With AMD

	Association With Smoking Years (Y)			
Variable	**Model Intercept [95% CI]**	**Slope [95% CI]**	***T* Value**	***P* Value**
BCVA (logMAR)	−0.36 [−0.69 to −0.02]	−0.0004 logMAR/y [−0.002 to 0.002]	−0.2	0.7
LLVA (logMAR)	−0.13 [−0.53 to 0.27]	−0.001 logMAR/y [−0.003 to 0.001]	−1.0	0.3
CS Gabor 3 cpd (logCS)	2.69 [1.34 – 4.04]	−0.004 logCS/y [−0.01 to 0.004]	−1.0	0.3
Metrics deduced from qCSF method				
CA (logCPD)	1.79 [1.34 – 2.24]	−0.001 logCPD/y [−0.004 to 0.001]	−1.0	0.3
AULCSF (logCS•logCPD)	2.14 [1.31 – 2.97]	−0.001 logCS•logCPD/y [−0.006 to 0.004]	−0.5	0.6
CS at specific spatial frequencies				
1 cpd (logCS)	1.99 [1.51 – 2.46]	−0.003 logCS/y [−0.006 to −0.0006]	−2.4	**0.02**
1.5 cpd (logCS)	2.19 [1.70 – 2.67]	−0.003 logCS/y [−0.006 to −0.0004]	−2.3	**0.03**
3 cpd (logCS)	2.37 [1.68 – 3.05]	−0.002 logCS/y [−0.006 to 0.002]	−1.2	0.3
6 cpd (logCS)	2.05 [1.09 – 3.0]	−0.00002 logCS/y [−0.005 to 0.005]	−0.01	1.0
12 cpd (logCS)	1.55 [0.47 – 2.64]	0.00018 logCS/y [−0.006 to 0.006]	0.06	1.0
18 cpd (logCS)	0.95 [0.16 – 1.74]	−0.002 logCS/y [−0.006 to 0.003]	−0.8	0.4

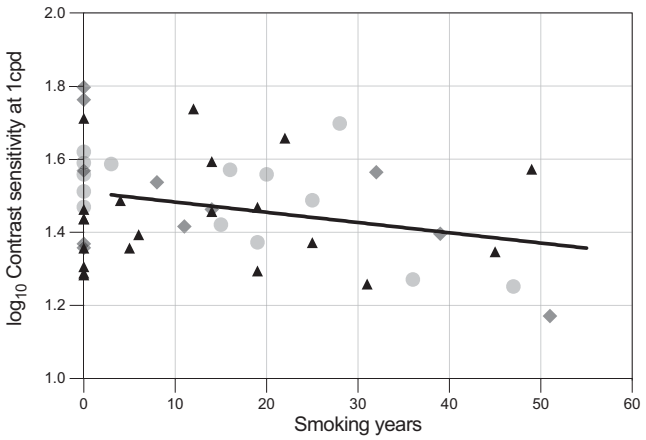

Figure 2. Relationship of CS at 1 CPD and smoking years. Linear model analysis reveals a significant association of CS at 1 CPD and smoking years. The Regression-line is plotted. Clear phakic eyes are represented by *circles*, pseudophakic eyes by *rhombs*, and eyes with mild cataract by *triangles*.

between the two groups. Only CS at 1 CPD and CS at 1.5 CPD revealed a significant difference between the eAMD and iAMD groups under mesopic lighting conditions. These findings suggest, that in trajectory from eAMD to iAMD CS decreases for stimuli, which only feature contrast changes at 1 to 1.5 cycles per degree. Considering the foveal diameter of about 0.8 mm and that 1 mm of retinal diameter accounts for 3.5 degrees of visual angle,[8] morphological correlates to these early functional deficits would include the foveal periphery up into the parafovea. These functional findings correspond to morphological data of Curcio and colleagues, who reported that age-related rod loss starts in the inferior parafovea[31] and that cones are more resilient than rods in the AMD disease trajectory.[32] With regard to drusen location, longitudinal studies with large study populations have described a concentration of drusen in the central ETDRS subfield in iAMD.[33,34] The drusen prevalence decreases by two thirds in the inner ring compared to the central subfield. Thus, the prevalence of drusen parallels the numerical distribution of cones in the retina. These findings at first sight contradict the described resilience of cones and vulnerability of rods in the AMD disease trajectory. However, xanthophyll-rich Müller glia cells have been proposed to exert an exclusively cone-protective effect.[8,35,36] Both xanthophyll content in the retina and Müller glia cells colocalize with cones and are concentrated in the central ETDRS subfield.[37–39] Rods do not benefit from this protection and hence perifoveal rods are more exposed to the harmful effects of high central drusen prevalence than cones. This proposed disease mechanism is compliant with the parafovea as the region of initial function loss, whereas the cone-rich fovea, even though exposed to higher drusen-prevalence, maintains functional capacities due to its protection. Further, the described mechanism would also explain the decrease of CS at lower spatial frequencies (CS at 1 CPD and CS at 1.5 CPD) in iAMD as follows. In the trajectory from eAMD to iAMD, there is no change in drusen localization. Rather, parafoveal rods, which contribute to CS at lower spatial frequencies, are subject to a drusen-associated functional decline, whereas the protected central cones, contributing to CS at higher spatial frequencies, persist. In addition to the considerations above, this cross-sectional analysis indicates that CS at low spatial frequencies (1 CPD and 1.5 CPD) is significantly associated with smoking years in patients with AMD. All other CS and VA metrics did not show noticeable associations with smoking years. Smoking has been reported to be associated with progression to advanced AMD.[23] However, to our knowledge, an association of smoking years to CS at specific spatial frequencies in AMD has yet not been described.

In conclusion, CS at 1 CPD and at 1.5 CPD are appealing candidates for the functional evaluation of AMD. Subsequent analysis of MUMOVI longitudinal data will further elicit their ability to detect a change in the trajectory toward advanced AMD, which is a prerequisite in establishing these metrics for therapeutic trials. Yet, measuring the whole CSF in this cross-sectional analysis is already of value, because it shows the diversity of functional candidate markers depending on the AMD stage. For interventional trials, it will be critical to select and predetermine specific qCSF-derived metrics to avoid type 2 errors resulting from compensation for multiple testing.

As the qCSF method has only been introduced recently, few comparable studies in AMD exist. Wai et al.[40] reported significant reductions of CS from 1 CPD to 6 CPD and for AULCSF in a dry AMD group without further subclassification compared to healthy controls. Ou et al.[16] described significant differences between control and respective AMD

groups (iAMD, AMD with subretinal drusenoid deposits, and geographic atrophy [GA]) for AULCSF and CS at 3 CPD in standard and low luminance qCSF. In addition, recently, Csaky[41] examined the qCSF method in the context of intermediate AMD, not detecting differences in AULCSF between "drusen-only" and "nascent GA." Our analysis is in line with these findings, even though the study designs do not match. With reference to the existing literature, our study adds new knowledge on CS in eAMD and iAMD.

In addition, we validated the qCSF measurements by also showing that contrast thresholds measured with Gabor patches, are significantly associated with all qCSF metrics. A model featuring CS at 3 CPD as the dependent variable and Gabor contrast threshold and age as fixed effects led to the best model fitting, which is intuitive, because contrast thresholds in Gabor patches are tested at a grating of 3 CPD. Spatial frequencies between 3 CPD and 5 CPD have become a standard for CS testing based on observations by Pelli et al.[17] and Legge et al.,[42] who proposed a preferential spatial frequency range to minimize the patient burden of time consuming chart-based testing. The above range was chosen, because it was found to be the optimum CS range in normal subjects and because it was shown to be essential for reading. At the same time, Pelli et al.[17] stated that it would be advantageous to conduct a detailed assessment of the whole CSF, if feasible. With the advent of the qCSF technology, researchers and clinicians now have an instrument at hand to reliably measure the full CSF in a reasonable time frame. This detailed CS testing method can provide functional markers, which classic CS testing methods would miss.

Several limitations to this study need to be considered. First, there is a significant difference in age between the control group and the AMD groups, respectively. As CS is significantly associated with age, this variable needed to be taken into account for analysis and was hence included as a fixed effect in linear models. In the MUMOVI data set, CS was also significantly associated with age. In contrast, the data did not provide an association between CS and lens status in the MUMOVI study cohort, which is likely due to the limitation of lenticular opacification in the inclusion criteria. Second, the study population comprises almost entirely white Europeans. Finally, this is a cross-sectional analysis. Longitudinal analyses are needed to describe the ability-to-detect change in CS metrics.

The qCSF method allows the detection of slight functional deficits in the AMD disease trajectory, which testing by Pelli-Robson charts would not identify. For example, we could describe a significant difference between AMD stages and a significant association between smoking years and CS at low spatial frequencies, which Pelli-Robson testing would have missed. Analyses like ours, which precisely measure the entire CSF, serve to describe candidate functional markers. This resource can be utilized in planning therapeutic trials, where a precise selection of markers is essential to avoid type 2 errors resulting from compensation for multiple testing.

Acknowledgments

The authors thank Leonie Schmidlin, Marc Repnow, Nils Schärer, and Daniela Hauenstein for their contributions to the study.

H.S. is supported by the Swiss National Science Foundation (Project funding: "Developing novel outcomes for clinical trials in Stargardt disease using structure/function relationship and deep learning" #310030_201165, and National Center of Competence in Research Molecular Systems Engineering: "NCCR MSE: Molecular Systems Engineering (phase II)" #51NF40-182895), the Wellcome Trust (PINNACLE study), and the Foundation Fighting Blindness Clinical Research Institute (ProgStar study). P.A. is supported by the foundation "Freiwillige Akademische Gesellschaft Basel" and the foundation "OPOS zugunsten von Wahrnehmungsbehinderten" (Project funding: "Validation of novel microperimetry metrics as functional outcome parameters for clinical trials targeting macular diseases"). The funding organizations had no role in the design or conduct of this research.

Disclosure: **P. Anders**, Bayer (F); **G.L. Traber**, None; **U. Hall**, None; **M. Pfau**, Apellis Pharmaceuticals (F, C), Novartis (R), Johnson & Johnson (C); **S.A. Garobbio**, None; **E.J. Chan**, None; **C. Gabrani**, None; **H. Camenzind**, Bayer (R), Apellis Pharmaceuticals (C); **M. Herzog**, None; **H. P. N. Scholl**, Astellas Pharma Global Development, Inc./Astellas Institute for Regenerative Medicine (C), Belite Bio (C), Boehringer Ingelheim Pharma GmbH & Co (C), Gerson Lehrman Group (C), Guidepoint Global, LLC (C), Janssen Research & Development, LLC (Johnson & Johnson) (C), Novo Nordisk (C), ReNeuron Group Plc/Ora Inc. (C), ReVision Therapeutics, Inc. (C), Stargazer Pharmaceuticals, Inc. (C), Tenpoint Therapeutics Ltd (C), Third Rock Ventures, LLC (C), Kinarus AG (F), Okuvision GmbH (F), Novartis Pharma AG (F)

References

1. Wong WL, Su X, Li X, et al. Global prevalence of age-related macular degeneration and disease burden projection for 2020 and 2040: a systematic review and meta-analysis. *Lancet Glob Health*. 2014;2(2):e106–e116.
2. Yehoshua Z, Wang F, Rosenfeld PJ, Penha FM, Feuer WJ, Gregori G. Natural history of drusen morphology in age-related macular degeneration using spectral domain optical coherence tomography. *Ophthalmology*. 2011;118(12):2434–2441.
3. Bogunovic H, Waldstein SM, Schlegl T, et al. Prediction of anti-VEGF treatment requirements in neovascular AMD using a machine learning approach. *Invest Ophthalmol Vis Sci*. 2017;58(7):3240–3248.
4. Bogunovic H, Montuoro A, Baratsits M, et al. Machine learning of the progression of intermediate age-related macular degeneration based on OCT imaging. *Invest Ophthalmol Vis Sci*. 2017;58(6):BIO141–BIO150.
5. Csaky K, Ferris F, Chew EY, Nair P, Cheetham JK, Duncan JL. Report from the NEI/FDA endpoints workshop on age-related macular degeneration and inherited retinal diseases. *Invest Ophthalmol Vis Sci*. 2017;58(9):3456–3463.
6. Lim LS, Mitchell P, Seddon JM, Holz FG, Wong TY. Age-related macular degeneration. *Lancet*. 2012;379(9827):1728–1738.
7. Lindner M, Nadal J, Mauschitz MM, et al. Combined fundus autofluorescence and near infrared reflectance as prognostic biomarkers for visual acuity in foveal-sparing geographic atrophy. *Invest Ophthalmol Vis Sci*. 2017;58(6):BIO61–BIO67.
8. Curcio CA, McGwin G, Sadda SR, et al. Functionally validated imaging endpoints in the Alabama study on early age-related macular degeneration 2 (ALSTAR2): design and methods. *BMC Ophthalmol*. 2020;20(1):196.
9. Vujosevic S, Pucci P, Casciano M, et al. Long-term longitudinal modifications in mesopic microperimetry in early and intermediate age-related macular degeneration. *Graefes Arch Clin Exp Ophthalmol*. 2017;255(2):301–309.

10. Pfau M, von der Emde L, Dysli C, et al. Light sensitivity within areas of geographic atrophy secondary to age-related macular degeneration. *Invest Ophthalmol Vis Sci*. 2019;60(12):3992–4001.
11. Wu Z, Ayton LN, Luu CD, Guymer RH. Relationship between retinal microstructures on optical coherence tomography and microperimetry in age-related macular degeneration. *Ophthalmology*. 2014;121(7):1445–1452.
12. Wu Z, Luu CD, Hodgson LAB, et al. Using microperimetry and low-luminance visual acuity to detect the onset of late age-related macular degeneration: a LEAD Study Report. *Retina*. 2021;41(5):1094–1101.
13. Pondorfer SG, Wintergerst MWM, Gorgi Zadeh S, et al. Association of visual function measures with drusen volume in early stages of age-related macular degeneration. *Invest Ophthalmol Vis Sci*. 2020;61(3):55.
14. Jindra LF, Zemon V. Contrast sensitivity testing: a more complete assessment of vision. *J Cataract Refract Surg*. 1989;15(2):141–148.
15. Hoffmann L, Rossouw P, Guichard MM, Hatz K. Strongest correlation between contrast sensitivity and morphological characteristics in bilateral nAMD. *Front Med (Lausanne)*. 2020;7:622877.
16. Ou WC, Lesmes LA, Christie AH, Denlar RA, Csaky KG. Normal- and low-luminance automated quantitative contrast sensitivity assessment in eyes with age-related macular degeneration. *Am J Ophthalmol*. 2021;226:148–155.
17. Pelli DG, Robson JG, Wilkins AJ. The design of a new letter chart for measuring contrast sensitivity. *Vision Research*. 1988;2(3):187–199.
18. McAnany JJ, Alexander KR. Spatial contrast sensitivity in dynamic and static additive luminance noise. *Vision Res*. 2010;50(19):1957–1965.
19. Tibber MS, Guedes A, Shepherd AJ. Orientation discrimination and contrast detection thresholds in migraine for cardinal and oblique angles. *Invest Ophthalmol Vis Sci*. 2006;47(12):5599–5604.
20. Ohlendorf A, Schaeffel F. Contrast adaptation induced by defocus - a possible error signal for emmetropization? *Vision Res*. 2009;49(2):249–256.
21. Hou F, Lesmes LA, Kim W, et al. Evaluating the performance of the quick CSF method in detecting contrast sensitivity function changes. *J Vis*. 2016;16(6):18.
22. Lesmes LA, Lu ZL, Baek J, Albright TD. Bayesian adaptive estimation of the contrast sensitivity function: the quick CSF method. *J Vis*. 2010;10(3):17.1–17.21.
23. Clemons TE, Milton RC, Klein R, Seddon JM, Ferris FL, Age-Related Eye Disease Study Research Group. Risk factors for the incidence of Advanced Age-Related Macular Degeneration in the Age-Related Eye Disease Study (AREDS) AREDS report no. 19. *Ophthalmology*. 2005;112(4):533–539.
24. Ferris FL, Wilkinson CP, Bird A, et al. Clinical classification of age-related macular degeneration. *Ophthalmology*. 2013;120(4):844–851.
25. Nasreddine ZS, Phillips NA, Bédirian V, et al. The Montreal Cognitive Assessment, MoCA: a brief screening tool for mild cognitive impairment. *J Am Geriatr Soc*. 2005;53(4):695–699.
26. Watson AB, Pelli DG. Quest: a Bayesian adaptive psychometric method. *Percept Psychophys*. 1983;33(2):113–120.
27. Traber GL, Della Volpe-Waizel M, Maloca P, et al. New technologies for outcome measures in glaucoma: review by the European Vision Institute Special Interest Focus Group. *Ophthalmic Res*. 2020;63(2):88–96.
28. R Core Team. (2014). *R: A language and environment for statistical computing*. Vienna, Austria: R Foundation for Statistical Computing. Accessed May 14, 2021. Available at: https://www.r-project.org/.
29. Brown VA. An introduction to linear mixed-effects modeling in R. *Adv Methods Pract Psychol Sci*. 2021;4(1): 2515245920960351.
30. Ying GS, Maguire MG, Glynn R, Rosner B. Tutorial on biostatistics: linear regression analysis of continuous correlated eye data. *Ophthalmic Epidemiol*. 2017;24(2):130–140.
31. Curcio C, Millican C, Allen K, Kalina R. Aging of the human photoreceptor mosaic: evidence for selective vulnerability of rods in central retina. *Invest Ophthalmol Vis Sci*. 1993;34:3278–3296.
32. Curcio CA. Photoreceptor topography in ageing and age-related maculopathy. *Eye (Lond)*. 2001;15(Pt 3):376–383.
33. Wang Q, Chappell RJ, Klein R, et al. Pattern of age-related maculopathy in the macular area. The Beaver Dam Eye Study. *Invest Ophthalmol Vis Sci*. 1996;37(11):2234–2242.
34. Chew EY, Clemons TE, Agrón E, et al. Ten-year follow-up of age-related macular degeneration in the age-related eye disease study: AREDS report no. 36. *JAMA Ophthalmol*. 2014;132(3):272–277.
35. Garlipp MA, Gonzalez-Fernandez F. Cone outer segment and Müller microvilli pericellular matrices provide binding domains for interphotoreceptor retinoid-binding protein (IRBP). *Exp Eye Res*. 2013;113:192–202.
36. Mata NL, Radu RA, Clemmons RC, Travis GH. Isomerization and oxidation of vitamin a in cone-dominant retinas: a novel pathway for visual-pigment regeneration in daylight. *Neuron*. 2002;36(1):69–80.
37. Syrbe S, Kuhrt H, Gärtner U, et al. Müller glial cells of the primate foveola: an electron microscopical study. *Exp Eye Res*. 2018;167:110–117.
38. Ahmad KM, Klug K, Herr S, Sterling P, Schein S. Cell density ratios in a foveal patch in macaque retina. *Vis Neurosci*. 2003;20(2):189–209.
39. Snodderly DM, Auran JD, Delori FC. The macular pigment. II. Spatial distribution in primate retinas. *Invest Ophthalmol Vis Sci*. 1984;25(6):674–685.
40. Wai KM, Vingopoulos F, Garg I, et al. Contrast sensitivity function in patients with macular disease and good visual acuity. *Br J Ophthalmol*. 2022;106(6):839–844.
41. Csaky KG. Cross-sectional study of cone function in age-related macular degeneration subjects with non-foveal nascent geographic atrophy. *Am J Ophthalmol*. 2023;247:25–34.
42. Legge GE, Pelli DG, Rubin GS, Schleske MM. Psychophysics of reading—I. Normal vision. *Vis Res*. 1985;25(2):239–252.

Investigative Ophthalmology & Visual Science